AMERICAN SOCIETY FOR MICROBIOLOGY | Molecular and Cellular Biology®

RESEARCH ARTICLE

SUMO-Modified FADD Recruits Cytosolic Drp1 and Caspase-10 to Mitochondria for Regulated Necrosis

Seon-Guk Choi, Hyunjoo Kim, Eun Il Jeong, Ho-June Lee, Sungwoo Park, Song-Yi Lee, Hyeon-Jeong Lee, Seong Won Lee, Chin Ha Chung, Yong-Keun Jung

Department of Biological Science, Seoul National University, Seoul, South Korea

ABSTRACT Fas-associated protein with death domain (FADD) plays a key role in extrinsic apoptosis. Here, we show that FADD is SUMOylated as an essential step during intrinsic necrosis. FADD was modified at multiple lysine residues (K120/125/149) by small ubiquitin-related modifier 2 (SUMO2) during necrosis caused by calcium ionophore A23187 and by ischemic damage. SUMOylated FADD bound to dynamin-related protein 1 (Drp1) in cells both *in vitro* and in ischemic tissue damage cores, thus promoting Drp1 recruitment by mitochondrial fission factor (Mff) to accomplish mitochondrial fragmentation. Mitochondrial-fragmentation-associated necrosis was blocked by FADD or Drp1 deficiency and SUMO-defective FADD expression. Interestingly, caspase-10, but not caspase-8, formed a ternary protein complex with SUMO-FADD/Drp1 on the mitochondria upon exposure to A23187 and potentiated Drp1 oligomerization for necrosis. Moreover, the caspase-10 L285F and A414V mutants, found in autoimmune lymphoproliferative syndrome and non-Hodgkin lymphoma, respectively, regulated this necrosis. Our study reveals an essential role of SUMOylated FADD in Drp1- and caspase-10-dependent necrosis, providing insights into the mechanism of regulated necrosis by calcium overload and ischemic injury.

KEYWORDS caspase-10, DRP1, FADD, necrosis, SUMOylation

Received 3 May 2016 **Returned for modification** 28 May 2016 **Accepted** 20 October 2016

Accepted manuscript posted online 31 October 2016

Citation Choi S-G, Kim H, Jeong EI, Lee H-J, Park S, Lee S-Y, Lee H-J, Lee SW, Chung CH, Jung Y-K. 2017. SUMO-modified FADD recruits cytosolic Drp1 and caspase-10 to mitochondria for regulated necrosis. Mol Cell Biol 37:e00254-16. https://doi.org/10.1128/MCB.00254-16.

Address correspondence to Yong-Keun Jung, ykjung@snu.ac.kr.

S.-G.C. and H.K. contributed equally to this work.

Programmed cell death (PCD) is typically classified into apoptosis and necrosis. Fas-associated protein with a death domain (FADD) is an essential adaptor in tumor necrosis factor (TNF) family-mediated extrinsic apoptosis, forming a death-inducing signaling complex (DISC) with death receptors and proximal caspases, such as caspase-10 and caspase-8. FADD also has a versatile role in cell proliferation and necroptosis, especially in extrinsic necrosis, by forming distinct protein complexes (1, 2). In contrast, many studies have revealed that FADD also has critical roles in caspase-independent intrinsic necrosis, but the mechanisms remain unknown (3, 4).

Owing to sequence homology with caspase-8, caspase-10 is hypothesized to be a component of DISC. However, studies investigating this hypothesis reported conflicting results (5, 6). Caspase-10 is also responsible for drug-induced intrinsic apoptosis in several types of cancer cells by forming the AK2/FADD/caspase-10 complex (7). Furthermore, caspase-10 inhibits autophagy through cleaving Bcl-2-associated transcription factor 1 (BCLAF1), a strong inducer of autophagy, and overexpressed caspase-10 activates the NF-κB pathway (8, 9). Interestingly, caspase-10 mutations are associated with autoimmune lymphoproliferative syndrome (ALPS) type II; other apoptosis-independent caspase-10 mutations were discovered in several primary tumors and in tumor cell lines from different origins (10–13). However, detailed characterization of the distinct roles of caspase-10 in cell death and in a range of pathologies is needed.

Accumulating evidence indicates that mitochondria are involved in regulated necrosis (14, 15). Mitochondrial integrity and function are closely connected; mitochon-

drial regulatory aberrations may occur in neurodegenerative diseases and in metabolic disorders (16, 17). During mitochondrial fission, dynamin-related protein 1 (Drp1) is translocated from the cytosol to the mitochondrial outer membrane, where it binds to mitochondrial Drp1 receptors and then oligomerizes to sever mitochondrial tubules (18, 19). Various stimuli result in excessive Drp1-mediated mitochondrial fragmentation, triggering necrotic cell death (20–22). However, the mechanisms by which Drp1 proteins are recruited to mitochondria and induce necrosis remain unclear.

The small ubiquitin-like modifier (SUMO) conjugation system utilizes a unique E1-activating (ubiquitin-activating) enzyme complex formed by (i) a heterodimer of SAE1 and SAE2 (Aos1/Uba2), (ii) the E2-conjugating enzyme Ubc9, and (iii) E3 ligases. Proteins of the SUMO family are reversibly deconjugated from the substrate by SUMO-specific isopeptidases (also known as sentrin-specific proteases [SENPs]) (23). SUMOylation has emerged as a posttranslational modification in several cell death pathways. Several proteins, including p53, NF-κB essential modulator (NEMO), and the caspases, are substrates for the SUMO conjugation system; this facilitates further exploration of SUMO protein involvement in cell death signaling (24–26). Here, we determined that SUMO2 is conjugated to nonconsensus lysine residues in FADD during necrosis. SUMOylated FADD is forced to translocate to the mitochondria together with Drp1 and caspase-10, leading to mitochondrial fragmentation and caspase-independent necrosis during hypoxic and ischemic injury.

RESULTS

FADD is modified by SUMO1 and SUMO2 *in vitro* and in necrotic cells. In an effort to elucidate whether FADD is a target of SUMOylation, we performed *in silico* modeling analyses. SUMO sp2.0 (a computing program with a group-based phosphorylation-scoring algorithm) predicted that Lys 125 (TKID) of FADD in the nonconsensus motif can be SUMOylated (27). To test this prediction, we first examined whether FADD could be modified by SUMO in cells. HEK-293T cells (human embryonic kidney 293 cells stably expressing the simian virus 40 [SV40] large T antigen) were cotransfected with hemagglutinin (HA)-tagged human FADD, along with FLAG-tagged Ubc9 (an E2 ligase) and His_6-tagged SUMO isoform 1 (SUMO1) or SUMO2. These transfections were performed in the presence of IDN-6556, an antiapoptotic pancaspase inhibitor, because FADD overexpression initiates apoptotic cell death. His_6-tagged, SUMO-conjugated proteins were isolated using Ni-nitrilotriacetic acid (NTA)-agarose beads under 5% SDS denaturing conditions and were mixed with *N*-ethylmaleimide to inhibit the action of SUMO proteases. Immunoblotting of the bead-bound proteins revealed a larger FADD protein (~50 kDa) that SUMOylated with SUMO2 more strongly than did HA-tagged FADD (~30 kDa) (Fig. 1A, top). SUMOylated FADD was also identified in cell lysates via immunoblot analysis (Fig. 1A, bottom).

We then analyzed whether FADD could be conjugated to SUMO2 *in vitro*. Recombinant GB1-tagged FADD protein was incubated with purified glutathione *S*-transferase (GST)-tagged SAE1/2 (E1), His_6-tagged Ubc9 (E2), and GST-tagged SUMO2 in the absence or presence of dithiothreitol (DTT). After incubation for increasing periods, samples were subjected to immunoblotting using an FADD antibody. Consistent with the results of *in vivo*-based experiments, *in vitro* incubation resulted in robust SUMO2 conjugation of FADD, as indicated by the high molecular masses (~80 kDa) (Fig. 1B). Similar results were observed in an *E. coli* SUMOylating system. His_6-FADD, E1, E2, and SUMOs were coexpressed by isopropyl β-D-1-thiogalactopyranoside (IPTG) treatment in *Escherichia coli* (28). Immunoblotting with an FADD antibody revealed a shifted band in lysates of bacteria that expressed His_6-FADD and either pT-E1E2SUMO1 or pT-E1E2SUMO2; this shifted band did not appear in the lysates of bacteria expressing FADD alone (Fig. 1C). To investigate which E3 SUMO ligases regulated FADD SUMOylation, four members of the protein inhibitor of activated STAT (PIAS) family, PIAS1, PIASx-α, PIAS3, and PIAS-γ, were each cotransfected with FADD and SUMO2 into HEK-293T cells. PIAS3 overexpression markedly increased FADD SUMOylation (Fig. 1D).

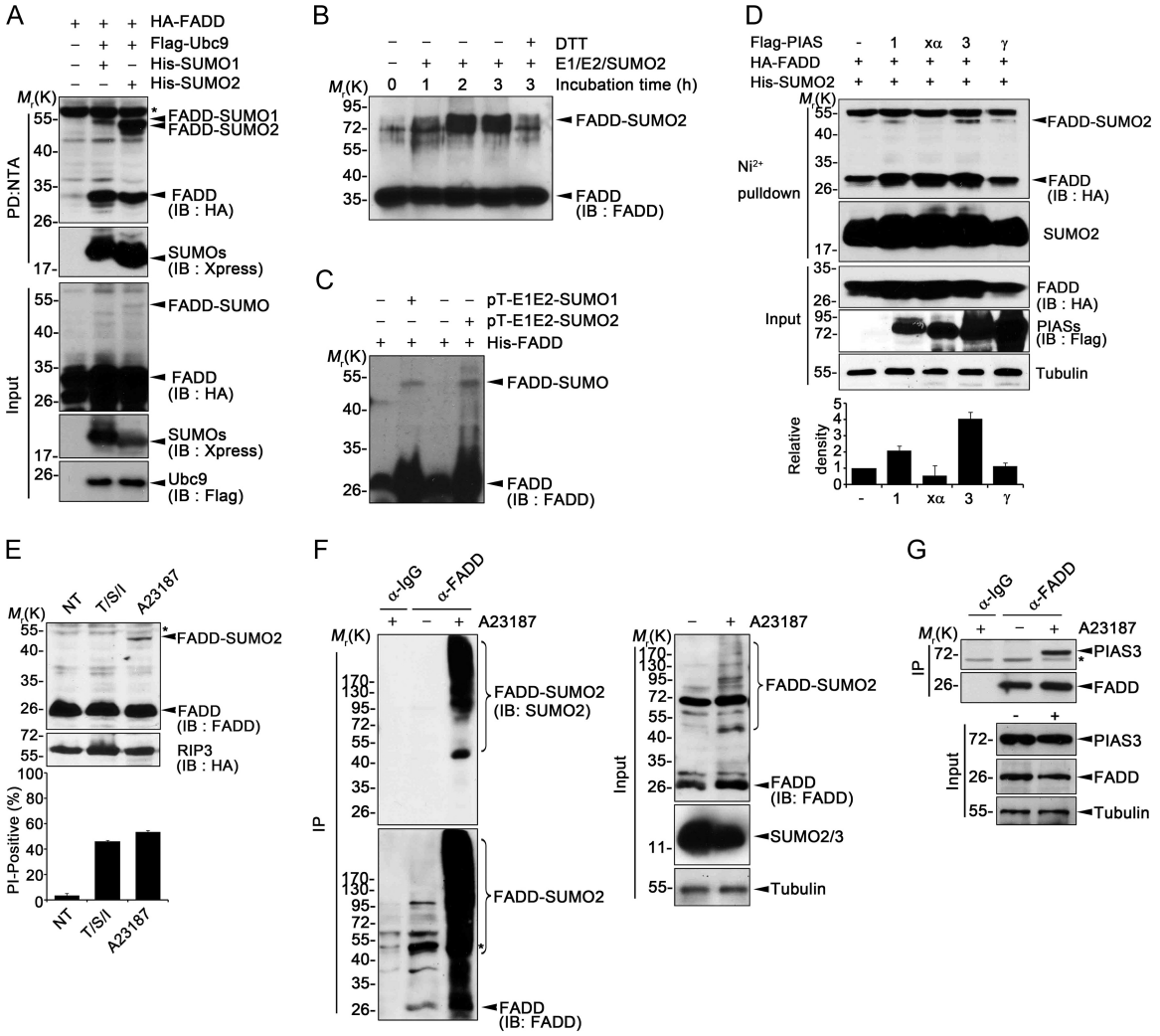

FIG 1 FADD is a target for SUMOylation during cell death. (A) (Top) HEK293T cells were transfected with HA-FADD alone or together with Flag-Ubc9 and His_6-SUMO1 or His_6-SUMO2 in the presence of 25 μM IDN. After 24 h, cell extracts were subjected to pulldown (PD) assays using Ni^{2+}-NTA-agarose beads under denaturing conditions, and the bound proteins were analyzed by immunoblot assay (IB). (Bottom) Whole-cell lysates (Input; 1/10) and the immunoprecipitates were immunoblotted with anti-HA, Xpress, and Flag antibodies. (B) Purified GB1-FADD protein was incubated with GST-Aos1/Uba2, His_6-Ubc9, and GST-SUMO2 (-GG), which has a deletion after GG in the C-terminal region of SUMO2 proteins in the presence of 100 μM DTT at 37°C and then subjected to immunoblot analysis. (C) *E. coli* BL21 cells were transformed with pET-FADD alone or in combination with pET-E1E2SUMO1 or pET-E1E2SUMO2 [which encode SUMO enzymes E1, E2, and SUMO1 or SUMO2 (-GG), respectively]. After 1 mM IPTG treatment for 6 h, the cell lysates were subjected to immunoblot analysis. (D) HEK-293T cells were cotransfected with HA-FADD, His-SUMO2, and either FLAG-PIAS1, FLAG–PIASx-α, FLAG-PIAS3, or FLAG–PIAS-γ in the presence of 25 μM IDN for 24 h. Cell extracts were then pulled down with Ni^{2+}-NTA-agarose beads as for panel A. (E) (Top) HeLa cells stably expressing HA-RIP3 were left untreated (NT) or treated with 40 ng/ml T/S/I for 6 h or 20 μM A23187 for 6 h and then subjected to immunoblot analysis. (Bottom) Cell death rates were determined by counting the PI-positive cells after staining with PI. (F) HeLa cells were treated with increasing concentrations of A23187 for 12 h (left) or with 20 μM A23187 for the indicated times (right). The cell lysates were subjected to immunoblot analysis. (G) HeLa cells were treated with 20 μM A23187 (+) for 4 h. Cell lysates were analyzed by IP assay with mouse IgG or anti-FADD antibody, followed by immunoblot analysis. The asterisks indicate nonspecific signals. Shown are mean values and standard deviations (SD) ($n \geq 3$).

To identify the cellular signals involved in FADD SUMOylation, we exposed HeLa cells to various insults to trigger different forms of apoptosis: (i) to trigger extrinsic apoptosis, we exposed the cells to TNF-α and cycloheximide or to FAS ligand; (ii) to trigger intrinsic apoptosis, we exposed the cells to etoposide or thapsigargin (29). We could not detect SUMOylated FADD under either of these conditions (see Fig. S1A in the supplemental material). We then examined FADD SUMOylation during necrotic cell death by treating HeLa cells expressing receptor-interacting serine/threonine-protein kinase 3 (HeLa/RIP3) with the combination of TNF-α, second mitochondrion-derived activator of caspases (SMAC) mimetic, and the pancaspase inhibitor IDN-6556 (T/S/I) to

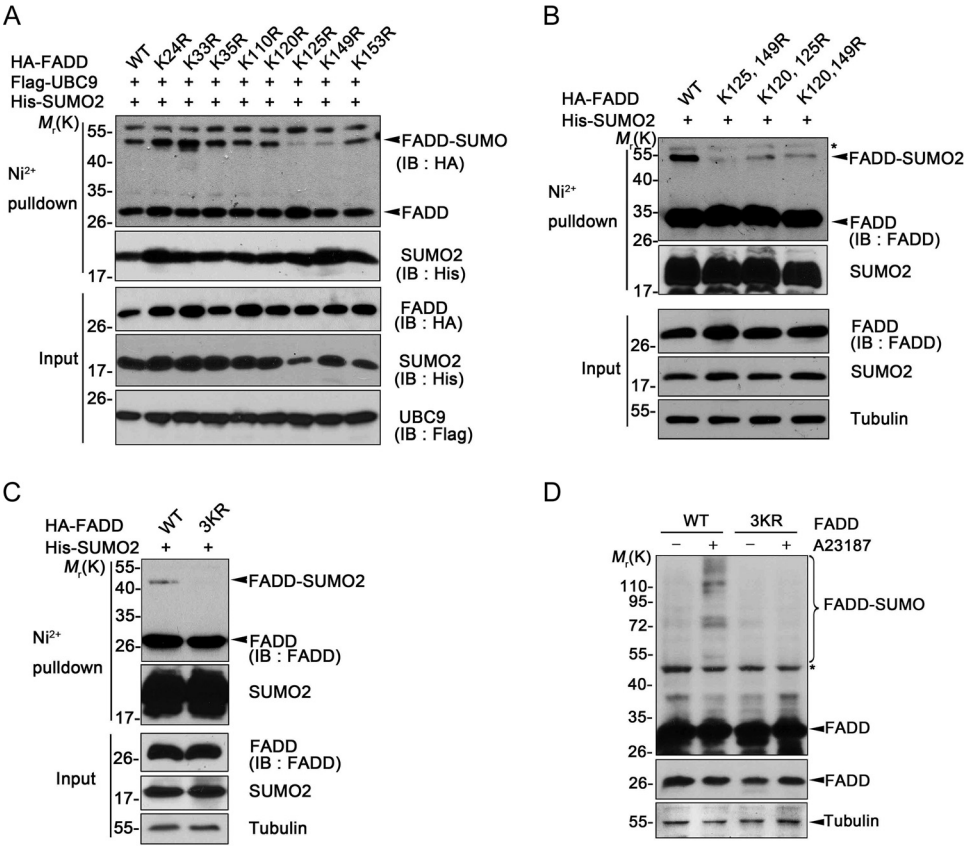

FIG 2 FADD is SUMOylated on lysines 120, 125, and 149. (A to C) Determination of FADD SUMOylation sites by mutagenesis. HEK-293T cells were cotransfected with Flag-Ubc9; His_6-SUMO2; and either HA-FADD WT, HA-FADD single Lys mutant (A), HA-FADD double Lys mutant (B), or HA-FADD triple Lys mutant (C) in the presence of 25 μM IDN. After 24 h, the cells were subjected to Ni^{2+} pulldown assay. The precipitates and whole-cell lysates (Input) were analyzed by immunoblotting. (D) HeLa cells were transfected with HA-FADD WT or HA-FADD K120/125/149R (3KR) mutant in the presence of 25 μM IDN for 24 h and then exposed to 20 μM A23187 for 6 h. The cell lysates were subjected to immunoblotting.

trigger necroptosis or a high dose of A23187 to induce intrinsic necrosis (15). Strikingly, FADD was conjugated to SUMO2 under high doses of A23187 but not by T/S/I treatment (Fig. 1E). SUMOylated FADD was observed in HeLa cells exposed to high doses ($>$5 μM) of A23187 but not in cells exposed to low doses ($<$2 μM) (see Fig. S1B in the supplemental material). In addition, FADD SUMOylation at high doses of A23187 increased for 6 h and then declined thereafter (see Fig. S1C in the supplemental material). From immunoprecipitation and immunoblot assays, we found apparently SUMOylated FADD in A23187-treated HeLa cells (Fig. 1F). Moreover, upon A23187 treatment, we found that FADD interacted with PIAS3 (Fig. 1G). These results suggest that FADD is SUMOylated during calcium-induced necrotic cell death.

FADD is SUMOylated at lysines 120, 125, and 149. To identify the SUMO-acceptable lysines in FADD, all eight lysine sites within FADD were replaced with arginines via mutagenesis. Pulldown assays that followed ectopic expression of FADD mutants, Ubc9, and SUMO2 revealed that mutation at lysine 125 (K125R) or 149 (K149R) in the death domain (DD) of FADD partially reduced the consequent incidence of SUMO-conjugated FADD (Fig. 2A). When we generated a FADD double mutant containing arginines at both lysines 125 and 149 (K125/149R) and combinations of proximal lysine 120 (K120/125R or K120/149R) the outcome was that FADD SUMOylation was greatly reduced but not completely abolished (Fig. 2B). Thus, we introduced one more mutation at lysine 120 into the FADD 2KR double mutant (K125/149R) and found that the FADD 3KR (K120/125/149R) triple mutation strongly impaired FADD SUMOylation (Fig. 2C). Accordingly, unlike the FADD 3KR (K120/125/149R) mutant (containing

triple mutations at lysines 120, 125, and 149), the FADD 3KR (K125/149/153R) mutant (harboring triple mutations at lysines 125, 149, and 153) was SUMOylated (see Fig. S2 in the supplemental material). In addition, when we treated HeLa cells with A23187 after ectopic expression of the FADD 3KR mutant, in contrast to the FADD wild type (WT), the FADD 3KR mutant was not SUMOylated (Fig. 2D). These results strongly suggest that FADD is modified by SUMO2 at lysines 125, 149, and 153 under excessive calcium overload.

SUMOylated FADD translocates to the mitochondria for Drp1-mediated mitochondrial fragmentation during necrosis. It was previously reported that calcium stress provokes translocation of the entire gamut of proapoptotic and necrogenic, cytoplasm-residual factors to the mitochondria. As reported previously (15, 30–32), we confirmed that upon A23187 treatment, both Drp1, a crucial regulator of mitochondrial fission (33), and p53 accumulated in the mitochondrion-rich fraction (Fig. 3A). Interestingly, we found that while A23187 treatment also increased FADD in the mitochondrion-rich fraction, it concomitantly reduced FADD in the cytosolic fraction. Of particular note, SUMOylated FADD was detected in the mitochondrial fraction 3 h after A23187 treatment (see Fig. S3A in the supplemental material). Immunocytochemical analysis also revealed that A23187 treatment increased the colocalization of FADD with TOM20 (translocase of outer membrane protein, subunit 20), a mitochondrial outer membrane protein; in contrast, untreated cells showed a cytosolic and diffused pattern of FADD localization (Fig. 3B). These results indicate that calcium stress causes FADD translocation to the mitochondria.

In general, excessive calcium influx (or overload) induces Drp1-dependent mitochondrial fragmentation. As previously reported (31), treatment of HeLa cells with A23187 increased the number of mitochondria showing fragmentation, with less elongated tubules (see Fig. S3B in the supplemental material). We thus examined whether FADD SUMOylation is critical to the mitochondrial fragmentation process. A23187-induced mitochondrial fragmentation and aggregate formation were greatly reduced in FADD knockout (KO) mouse embryo fibroblasts (MEFs) (Fig. 3C, left), compared to observations of FADD WT MEFs. The number of cells with fragmented mitochondria was reduced from 60% to 20% by FADD deficiency (Fig. 3C, right). In addition, FADD KO MEFs expressing the SUMOylation-defective FADD 3KR mutant underwent approximately 30% less mitochondrial fragmentation than did FADD KO MEFs expressing FADD WT under calcium overload (Fig. 3D). These observations indicate that SUMOylated FADD is required for mitochondrial fragmentation under calcium overload.

Under excessive calcium overload, Drp1-dependent mitochondrial fission mediates not only apoptosis (34) but also necrosis (15), depending on the duration or concentration of the overload (35, 36). We determined the types of cell death evoked by A23187 in detail. Cell death induced by low doses (<2 μM) of A23187 was efficiently inhibited by the caspase inhibitor IDN-6556. In contrast, cell death triggered by high doses (>5 μM) of A23187 was not inhibited, but rather, was potentiated by IDN-6556 (see Fig. S4A in the supplemental material). Accordingly, caspase-8 and caspase-9 were not activated (see Fig. S4C), mitochondrial cytochrome *c* was not released into the cytosol (see Fig. S4B), and cellular ATP levels were reduced by treatment with 20 μM A23187 (see Fig. S4D). These results confirm that high doses of A23187 induce caspase-independent necrosis. Furthermore, using the calcein/cobalt-bleaching assay, we found that 20 μM A23187 did not affect mitochondrial permeability transition pore (MPTP) opening, nor did it affect mitochondrial permeability transition (mPT) in both FADD WT and FADD KO MEFs (see Fig. S5), indicating that A23187-induced necrosis is independent of mPT.

When we addressed whether FADD and Drp1 are required for A23187-induced necrosis, we found that either FADD or Drp1 deficiency in MEFs greatly blocked necrotic cell death, as measured by propidium iodide (PI) staining (Fig. 3E). Accordingly, unlike in WT MEFs, MEFs with FADD-deficient mutations or Drp1-deficient mutations eliminated the necrosis-indicating reduction of cellular ATP levels normally caused by

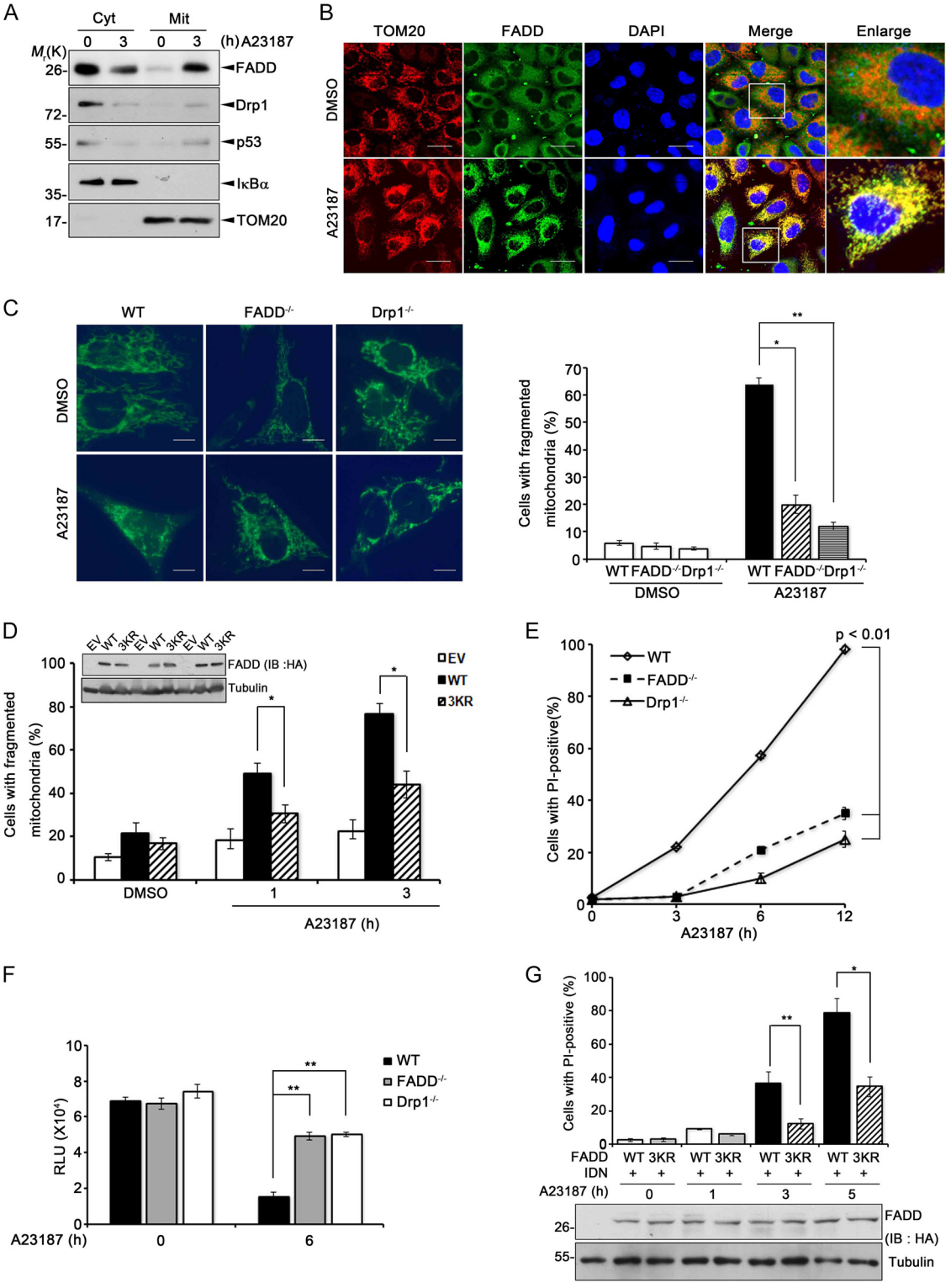

FIG 3 SUMOylated FADD is recruited to the mitochondria for mitochondrial fragmentation during necrotic cell death. (A) After treatment with 20 μM A23187 for 3 h, cytosolic (Cyt) and mitochondrial (Mit) fractions of HeLa cells were prepared and analyzed by immunoblot assay. (B) HeLa/Mito-RFP (red fluorescent protein) cells were treated with DMSO (vehicle) or 10 μM A23187 for 3 h and then analyzed by immunocytochemical assay. Nuclei were stained with DAPI (4′,6-diamidino-2-phenylindole). Scale bars, 20 μm. (C) WT, FADD$^{-/-}$, and Drp1$^{-/-}$ MEFs were transfected with mitotracker (mito-GFP) for 24 h and treated with 20 μM A23187 for 3 h. Mitochondrial fragmentation ratios were determined by counting the cells showing fragmented mitochondria among total GFP-positive cells (each group, >100 cells). *, $P < 0.05$; **, $P < 0.01$. Scale bars, 10 μm. (D) FADD$^{-/-}$ MEFs were transfected with mito-GFP and pcDNA (EV), HA-FADD WT, or HA-FADD K120/125/149R mutant (3KR) for 24 h and then exposed to 10 μM A23187 for 3 h. The mitochondrial fragmentation assay was assessed as for panel C. *, $P < 0.05$. (Inset) The cell lysates were examined by Western blotting.

(Continued on next page)

A23187 treatment (Fig. 3F). Furthermore, we investigated the necessity of FADD SUMO modification in A23187-induced necrosis. While ectopic expression of FADD WT potentiated A23187-induced necrosis, the FADD 3KR mutant showed a 4-fold-lower stimulatory effect than FADD WT on A23187-induced necrosis at 3 h (Fig. 3G). In addition, cell death triggered by A23187 was significantly suppressed by knockdown of PIAS3 expression (see Fig. S6 in the supplemental material). In summary, these results demonstrate that SUMO-modified FADD is required for caspase-independent necrotic cell death.

SUMOylated FADD interacts with Drp1 to promote Drp1 translocation to mitochondria. Since we observed that Drp1 accumulated on the mitochondria upon A23187 treatment and also observed that FADD was required for mitochondrial fragmentation, we hypothesized that FADD-mediated mitochondrial fragmentation might depend on Drp1 activity. To test this hypothesis, we examined the effects of the Drp1 K38A dominant-negative mutant, which lacks GTPase activity and thus prevents Drp1 translocation to the mitochondria upon mitochondrial fragmentation. As expected, ectopic expression of the Drp1 K38A mutant abolished FADD-induced mitochondrial fragmentation in HeLa cells (Fig. 4A). We then addressed how FADD functionally regulated Drp1 activity. Immunoprecipitation assays indicated that FADD interacted with Drp1 in the mitochondrial and cytosolic fractions of cells treated with A23187 but not in those of untreated cells (Fig. 4B). In addition, the results of *in vitro* binding assays using combinations of purified proteins illustrated that SUMOylated FADD presented a much higher affinity for Drp1 protein than did unmodified FADD (Fig. 4C). Furthermore, as observed for endogenous FADD, immunoprecipitation assays showed that the HA-FADD WT interacted with Drp1 in the mitochondrial fractions of HeLa cells that had been treated with A23187. In contrast, the FADD 3KR mutant failed to interact with Drp1 regardless of A23187 treatment (Fig. 4D). These observations suggest that SUMOylated FADD interacts with Drp1 during mitochondrial fragmentation.

When we addressed which mitochondrial Drp1 receptor/adaptor is utilized for FADD/Drp1-mediated mitochondrial fragmentation, we found that mitochondrial fission factor (Mff) bound to FADD under calcium stress but that other receptors, such as Fis1, MiD49, and MiD51, did not (Fig. 4E). Drp1 was also detected in the same protein complex by immunoprecipitation assay. We then questioned whether FADD was required for Drp1 recruitment to the mitochondria. The results from fractionation assays revealed that, in contrast to WT MEFs, lack of FADD expression in MEFs apparently reduced Drp1 recruitment into the mitochondrial fraction after cells had been treated with A23187 (Fig. 4F). These results indicate that FADD, especially SUMOylated FADD, contributes to Drp1 recruitment onto the mitochondria, probably by utilizing Mff in response to calcium overload.

FADD SUMOylation is required for hypoxic cell death. Both excessive calcium influx and intracellular accumulation of calcium (resulting in overload) are frequently observed under ischemic and hypoxic conditions (37). We examined FADD SUMOylation and its role in a physiological model of hypoxia. Immunoblot analysis revealed that FADD was SUMOylated in HeLa cells after 24 h of hypoxia (conditions where O_2 is $\leq$1%) (Fig. 5A). In contrast, chelation of intracellular Ca^{2+} with a calcium-binding compound, BAPTA-AM, prevented hypoxia-induced FADD SUMOylation, indicating that calcium plays a critical role in FADD SUMOylation under hypoxia. In addition, FADD SUMOylation was reduced at 4 h after reoxygenation following hypoxia (Fig. 5B). As in cells that had been exposed to A23187, we could also detect SUMOylated FADD in the mitochondrion-rich fraction of cells that had been exposed to hypoxic conditions for 24

FIG 3 Legend (Continued)
(E) FADD WT, FADD$^{-/-}$, and Drp1$^{-/-}$ MEFs were treated with 20 μM A23187 for the indicated times, and cell death rates were determined by counting the PI-positive cells. (F) Cells were treated as described for panel E, and cellular ATP levels were measured. **, $P < 0.01$. (G) FADD$^{-/-}$ MEFs were pretreated with 25 μM IDN for 3 h and then cotransfected with pEGFP and FADD WT or FADD K120/125/149R (3KR) mutant in the presence of 25 μM IDN for 24 h. After treatment with 20 μM A23187, cell death rates were determined as for panel E. *, $P < 0.05$; **, $P < 0.01$. Shown are mean values and SD ($n \geq 3$).

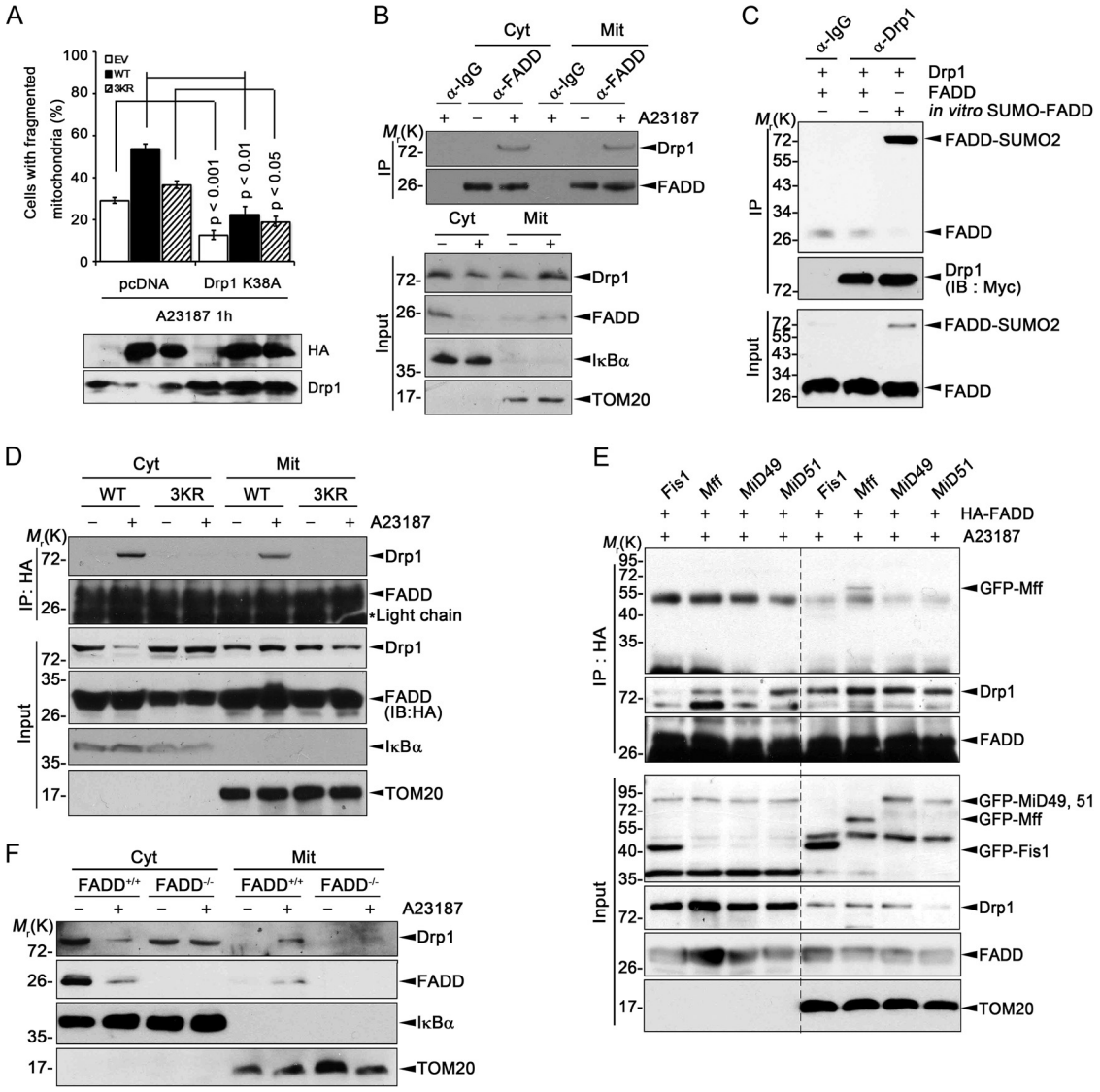

FIG 4 FADD SUMOylation is essential for interaction with Drp1 and mitochondrial recruitment of Drp1. (A) HeLa/Mito-RFP cells were cotransfected with FADD WT, alone or together with the Drp1 K38A mutant, in the presence of 25 μM IDN. (Bottom) After 24 h, the cells were incubated with 10 μM A23187 for 1 h and analyzed by immunoblotting. (Top) A mitochondrial fragmentation assay was assessed as for Fig. 3C (each group, >100 cells). Shown are mean values and SD ($n \geq 3$). (B) After treatment with 20 μM A23187 for 3 h, cytosolic and mitochondrial fractions of HeLa cells were analyzed by IP assay using anti-FADD antibody (top) or input was examined by immunoblotting (bottom). (C) (Top) Purified Myc-Drp1 protein was incubated with *in vitro* SUMOylated His_6-FADD and native His-FADD protein, and the reaction mixtures were then subjected to IP assay using anti-Drp1 antibody. (Bottom) Immunoprecipitates and input were analyzed by immunoblotting. (D) HeLa cells were transfected with either HA-FADD WT or HA-FADD K120/125/149R (3KR) mutant in the presence of 25 μM IDN for 24 h and treated with 10 μM A23187 for 1 h. Cytosolic and mitochondrial fractions were analyzed by IP assay using anti-HA antibody. (E) HeLa cells were cotransfected with HA-FADD and GFP-Fis1, GFP-Mff, GFP-MiD49, or GFP-MiD51 in the presence of 25 μM IDN for 24 h. After treatment with 20 μM A23187 for 3 h, cytosolic and mitochondrial fractions were subjected to IP assay using anti-HA antibody. (F) $FADD^{+/+}$ and $FADD^{-/-}$ MEFs were treated with 20 μM A23187 for 3 h. Cytosolic and mitochondrial fractions were analyzed by immunoblotting.

and 48 h (Fig. 5C). We then investigated whether FADD is required for cell death during hypoxia. FADD knockdown in HeLa cells significantly inhibited mitochondrial fragmentation under hypoxic conditions (Fig. 5D) and reduced hypoxia-induced cell death (Fig. 5E). Hypoxia-induced cell death was further suppressed in FADD knockdown in HeLa cells treated with a caspase inhibitor (Fig. 5E), indicating that FADD is a key regulator of necrosis.

When we examined FADD SUMOylation in the mouse brain after ischemic injury from middle cerebral artery occlusion (MCAO), we found that mouse FADD was SUMOylated in the ischemic damage core but not in the nonischemic contralateral region (Fig. 5F). While

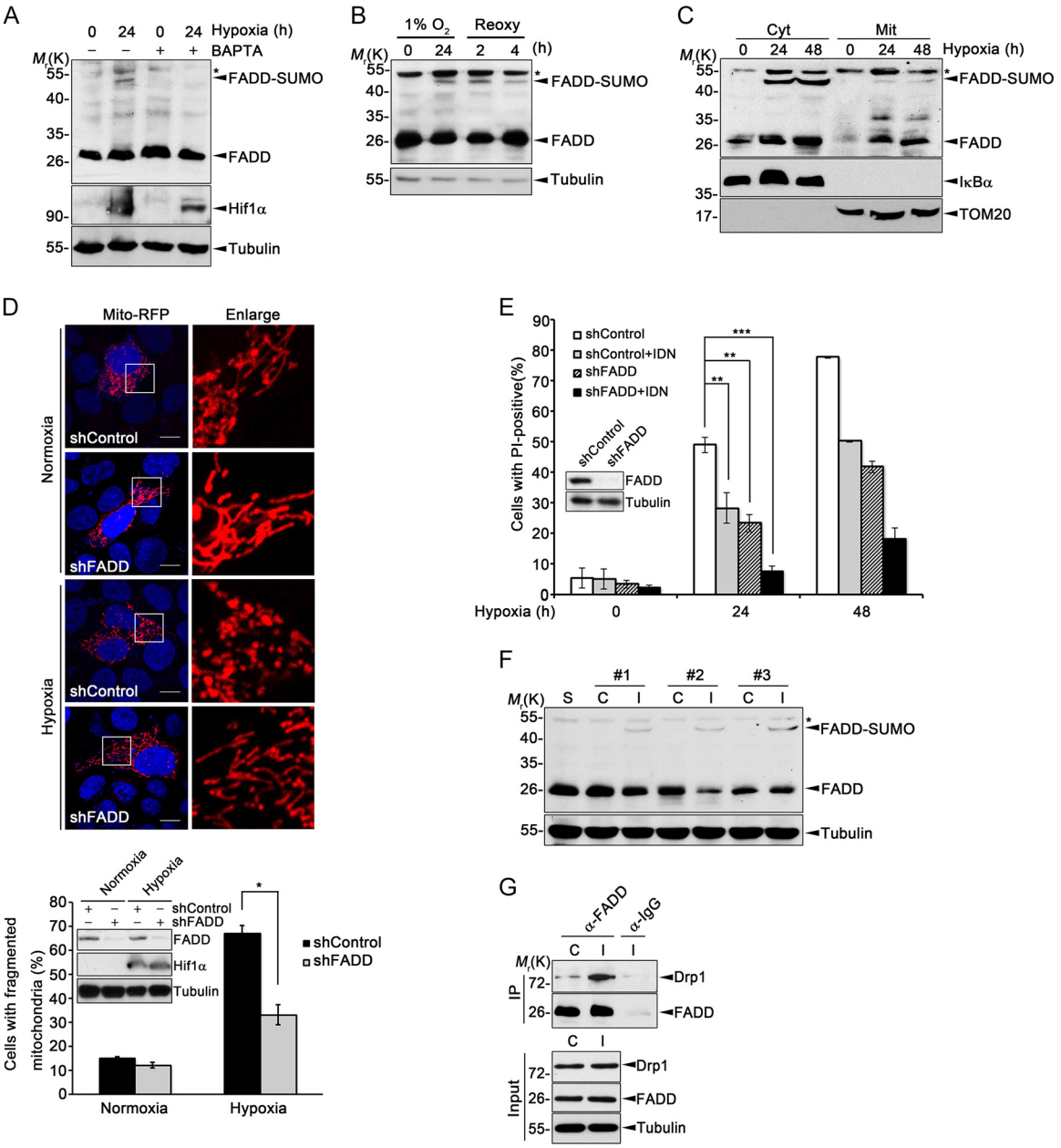

FIG 5 FADD is SUMOylated and interacts with Drp1 during ischemic stroke. (A) HeLa cells were exposed to normoxic (20% O_2) or hypoxic (1% O_2) conditions in the presence of 10 μM BAPTA-AM for the indicated periods. Cell extracts were analyzed by immunoblotting using anti-FADD antibody. (B) HeLa cells were exposed to experimental normoxia, hypoxia, and hypoxia-reoxygenation (Reoxy) (subsequently exposed to 20% O_2) for the indicated periods. Cell extracts were analyzed by immunoblotting. (C) HeLa cells were incubated under hypoxic conditions for the indicated times, and cytosolic and mitochondrial fractions were analyzed by immunoblotting. (D) HeLa cells were cotransfected with pEGFP, mito-RFP, and either pSUPER.neo (shControl) or FADD shRNA (shFADD) for 48 h and then exposed to hypoxia for 24 h. Mitochondrial morphology in GFP-positive cells (at least 100 cells per group) was analyzed by fluorescence microscopy (top), and percentages of mitochondrial fragmentation were determined (bottom). (Inset) Cell extracts were analyzed by immunoblotting. *, $P < 0.05$. Scale bars, 10 μm. (E) HeLa cells were transfected with pEGFP and either pSUPER.neo (shControl) or FADD shRNA (shFADD) for 48 h. The cells were then exposed to hypoxia in the presence of 25 μM IDN, and cell death rates were determined after staining with PI. **, $P < 0.01$; ***, $P < 0.001$. Shown are mean values and SD ($n \geq 3$). (F and G) Three-month-old male BALB/c mice were subjected to MCAO for 30 min as described in Materials and Methods. Brain lysates (except the cerebellum) were then prepared from the nonischemic (contralateral [C]), ischemic (ipsilateral [I]), and sham control (S) hemispheres and subjected to immunoblotting (F) or IP assay using anti-FADD antibody (G). The immunoprecipitates and whole-cell lysates (Input) were analyzed by immunoblotting.

the expression levels of FADD and Drp1 were unchanged, immunoprecipitation assays showed that ischemic damage in the mouse brain increased the interaction of FADD and Drp1 in the ischemic damage core (Fig. 5G). These results indicate that FADD is SUMOylated and interacts with Drp1in the mouse brain during ischemic injury.

Caspase-10 forms a ternary protein complex with SUMO-FADD/Drp1 for necrosis. Since FADD is known to bind to proximal caspases, such as caspase-8 and casepase-10, we examined a possible role for these caspases in A23187-induced necrosis. Using short hairpin RNAs (shRNAs), we reduced the protein levels of FADD, caspase-8, and caspase-10 (Fig. 6A). To our surprise, we found that the caspase-10 knockdown, but not the caspase-8 knockdown, blocked A23187-induced cell death as much as the FADD knockdown did (Fig. 6B). When we examined subcellular localization of caspase-10 during cell death, it was detected in both the mitochondrial and cytosolic fractions of cells that had undergone treatment with A23187 (Fig. 6C). Consistently, deficiency of caspase-10 but not caspase-8 also inhibited A23187-induced mitochondrial fragmentation (Fig. 6D; see Fig. S7 in the supplemental material). These results indicate that caspase-10 is required for A23187-induced necrosis.

In addition, immunoprecipitation assays revealed that caspase-10 was recruited into the FADD/Drp1 complex in FADD WT MEFs upon A23187 treatment (Fig. 6E). Owing to the lack of caspase-10 in the WT mouse, MEFs were transfected with human caspase-10. However, this caspase-10/FADD/Drp1 complex was not observed in FADD knockout MEFs (Fig. 6E), indicating that FADD is required for the formation of the caspase-10/FADD/Drp1 complex. Notably, *in vitro* binding assays clearly showed that purified caspase-10 protein formed a ternary protein complex with SUMOylated FADD and myc-Drp1 (Fig. 6F). Moreover, immunoprecipitation assays showed that caspase-10 interacted with FADD and Drp1 only in the mitochondrion-rich fraction but not in the cytosolic fraction of cells that had undergone A23187 treatment (Fig. 6G). In contrast, caspase-8 was not observed in the FADD-Drp1 protein complex. These observations strongly indicate that caspase-10 forms a protein complex with SUMOylated FADD/Drp1 on the mitochondrial membrane during necrosis.

Caspase-10 mutants identified in human diseases regulate Drp1 oligomerization and necrosis differently. According to the results shown in Fig. 6G, A23187 treatment induced the formation of highly ordered oligomeric Drp1—an active form of Drp1 for mitochondrial fission (38)—in the mitochondrial fraction. To evaluate the possible role of caspase-10 in A23187-induced mitochondrial fragmentation, we assessed the effects of its knockdown on Drp1 oligomerization. Western blotting under nonreducing conditions revealed that reduction of caspase-10 expression significantly abrogated A23187-induced Drp1 oligomerization in A23187-treated HeLa cells (Fig. 7A). In contrast, inhibition of Drp1 oligomerization was not significantly affected by the caspase-8 knockdown. Conversely, ectopic expression of caspase-10 in the MCF-7 human breast cell line, which normally does not express caspase-10, markedly increased the level of oligomeric Drp1 (Fig. 7B, top) and necrosis (Fig. 7B, bottom). Ectopic expression of caspase-10 in cells exposed to A23187 had the same effects. These results indicate that caspase-10 might regulate Drp1 oligomerization for mitochondrial fragmentation during necrosis.

Previous studies showed that in autoimmune lymphoproliferative syndrome (ALPS) type II, non-Hodgkin lymphoma, and gastric cancer, five mutations of caspase-10 (V410I, L285F, L24I, A414V, and V491L) impair apoptosis (11–13). The notion that caspase-10 is crucial for necrosis led us to evaluate the activities of these capspase-10 mutants in FADD/Drp1-mediated mitochondrial fragmentation and necrosis. Consistent with the previous reports, overexpression analyses revealed that all of the caspase-10 mutants significantly blocked apoptosis induced by TNF-related apoptosis-inducing ligand (TRAIL) (Fig. 7C). As could be expected, A23187-induced mitochondrial fragmentation was accelerated by ectopic expression of caspase-10 WT. Interestingly, the caspase-10 L285F and V414L mutants displayed distinct activities on mitochondrial fragmentation in the cells treated with A23187 (Fig. 7D). The caspase-10 L285F mutant, which is detected in ALPS type II (13), more potently increased mitochondrial fragmentation; the caspase-10 A414V mutant, which is mainly detected in non-Hodgkin lymphoma (12), was less effective in inducing mitochondrial fragmentation than caspase-10 WT. Furthermore, the caspase-10 L285F mutant greatly increased Drp1 oligomerization in the transfected MCF7 cells, and the caspase-10 A414V mutant was

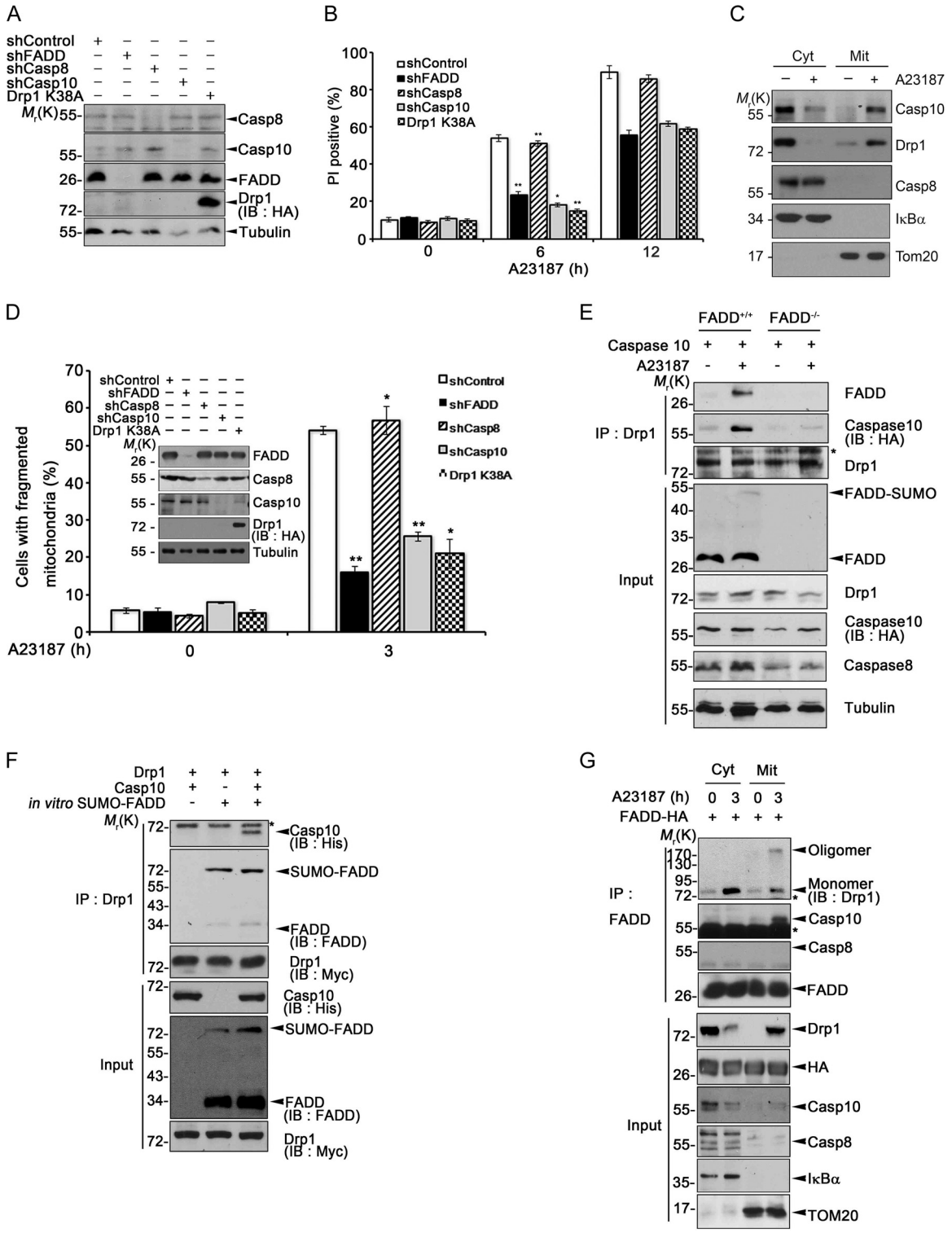

FIG 6 Caspase-10 is essential for necrosis and forms a ternary protein complex with SUMO-FADD/Drp1. (A and B) HeLa cells were transfected with FADD-targeting shRNA, caspase-8-targeting shRNA, caspase-10-targeting shRNA, or Drp1 K38A mutant, together with GFP, for 48 h and treated with 20 μM A23187 for the indicated times. (A) The cells were analyzed for expression of the proteins by immunoblotting. (B) After staining with PI, cell death rates were measured as described in the legend to Fig. 3. *, $P < 0.05$; **, $P < 0.01$. (C) HeLa cells were left untreated or were treated with 20 μM A23187. Mitochondrial and cytoplasmic fractions were analyzed via immunoblotting using anti-caspase-10 antibody. (D) HeLa cells were transfected with FADD-targeting shRNA, caspase-8-targeting shRNA, caspase-10-targeting shRNA, or Drp1 K38A mutant, together with mito-RFP. After 48 h, the cells were treated with 10 μM A23187 for 2 h. Mitochondrial morphology in RFP-positive cells was analyzed by fluorescence microscopy, and the percentages of cells (from a sample of at least 100) showing fragmented mitochondria were determined. *, $P < 0.05$; **, $P < 0.01$. (Inset) Cell lysates were analyzed by Western blotting. (E) FADD$^{+/+}$ and FADD$^{-/-}$ MEFs were transfected with caspase-10 for 24 h and then treated with 20 μM A23187 for 3 h. The

(Continued on next page)

less effective than caspase-10 WT (Fig. 7E). Consistent with their effects on mitochondrial fragmentation, the caspase-10 L285F mutant potentiated A23187-induced necrotic cell death, while the caspase-10 A414V mutant was less effective than caspase-10 WT (Fig. 7F). These results suggest that caspase-10 mutations observed in human diseases might distinctly regulate necrosis through Drp1 oligomerization independently of their apoptosis-modulating activity.

DISCUSSION

SUMOylation mostly occurs at the consensus motif Ψ-K-X-D/E (where Ψ is a hydrophobic residue, K is the lysine conjugated to SUMO, X is any amino acid, and D or E is an acidic residue) in target proteins via the action of a single E2 enzyme (UBC9) (39). According to our observations, three lysine residues (Lys120, Lys125, and Lys149) in the FADD death domain contribute to its SUMO modification; the sequences surrounding the three lysines in FADD, $_{119}$LKVS$_{122}$, $_{124}$TKID$_{127}$, and $_{148}$WKNT$_{151}$, are not consistent with the canonical SUMOylation motif. Recent evidence extends this consensus SUMO acceptor motif to two additional exceptions, the phosphorylation-dependent SUMOylation motif (PDSM) and the negatively charged amino acid-dependent SUMOylation motif (NDSM) (40). While phosphorylation at the serine 198 residue in human FADD occurs upon signaling, both the FADD phosphomimic and the FADD-dead mutant are also conjugated with SUMO2 (data not shown). Thus, the lysine residues in FADD also do not coincide with PDSM. In some cases, SUMO acceptor lysines, such as the Lys14-containing SUMO acceptor site ($_{13}$FKEW$_{16}$) in the human ubiquitin conjugation enzyme E2-25K, do not require acidic residues for their SUMOylation but are recognized in the context of a stable α-helix (40). Similarly, the three lysines in FADD are part of an α-helix and are in close proximity to the secondary structure. While a single mutation at lysine 120 did not affect FADD SUMOylation, we found that, compared to triple mutations at lysines 125, 149, and 153, triple mutations at lysines 120, 125, and 149 abolished FADD SUMOylation. This might be due to compensatory conjugations at the proximal lysine 120 when both lysine 125 and 149 were mutated.

Among SUMOylation-induced regulations, altered functions in apoptosis were reported in a few cases (41–43). While FADD was recently reported to participate in necroptosis as a negative regulator after its ubiquitination (2), we did not observe FADD SUMOylation in apoptosis or in necroptosis. In the past decade, the concept of "regulated necrosis" has generated considerations of more—and different—forms of necrotic cell death, such as necroptosis, ferroptosis, oxytosis, ETosis, NETosis, cyclophilin D (CypD)-mediated regulated necrosis, and pyroptosis, all based on their initiating mechanisms. The best-studied model of regulated necrosis is probably necroptosis. In general, TNF-induced necroptosis is initiated by the kinase activities of RIPK1 and RIPK3, and this necrosis is promoted by lack of FADD or lack of caspase-8. In contrast, calcium overload-induced necrosis at least does not require RIP3 and was rather suppressed by a lack of FADD. Similar RIPK1/RIPK3-independent necrosis is also found in CypD-mediated regulated necrosis during H_2O_2 treatment and *Shigella flexneri* infection (44). However, this calcium overload-induced necrosis is different from CypD-mediated regulated necrosis in that calcium overload disrupts mitochondria before the CypD-dependent mitochondrial permeability transition pore opening occurs. We propose that calcium overload-induced necrosis is mediated by SUMOylated FADD independently of RIP3.

We found this type of cell death in Ca^{2+} overload/hypoxia-induced necrosis, which

FIG 6 Legend (Continued)
cell lysates were subjected to IP assay using anti-Drp1 antibody. (F) Purified Myc-Drp1 protein was incubated with *in vitro* SUMOylated His_6-FADD and His–caspase-10 proteins, followed by IP assay using anti-Drp1 antibody. (G) HeLa cells were transfected with FADD-HA for 24 h cells in the presence of 25 μM IDN and were then treated with 20 μM A23187 for 3 h. Cytosolic and mitochondrial fractions were subjected to IP assay using anti-FADD antibody, followed by immunoblotting under nonreducing conditions. Shown are mean values and SD ($n \geq 3$).

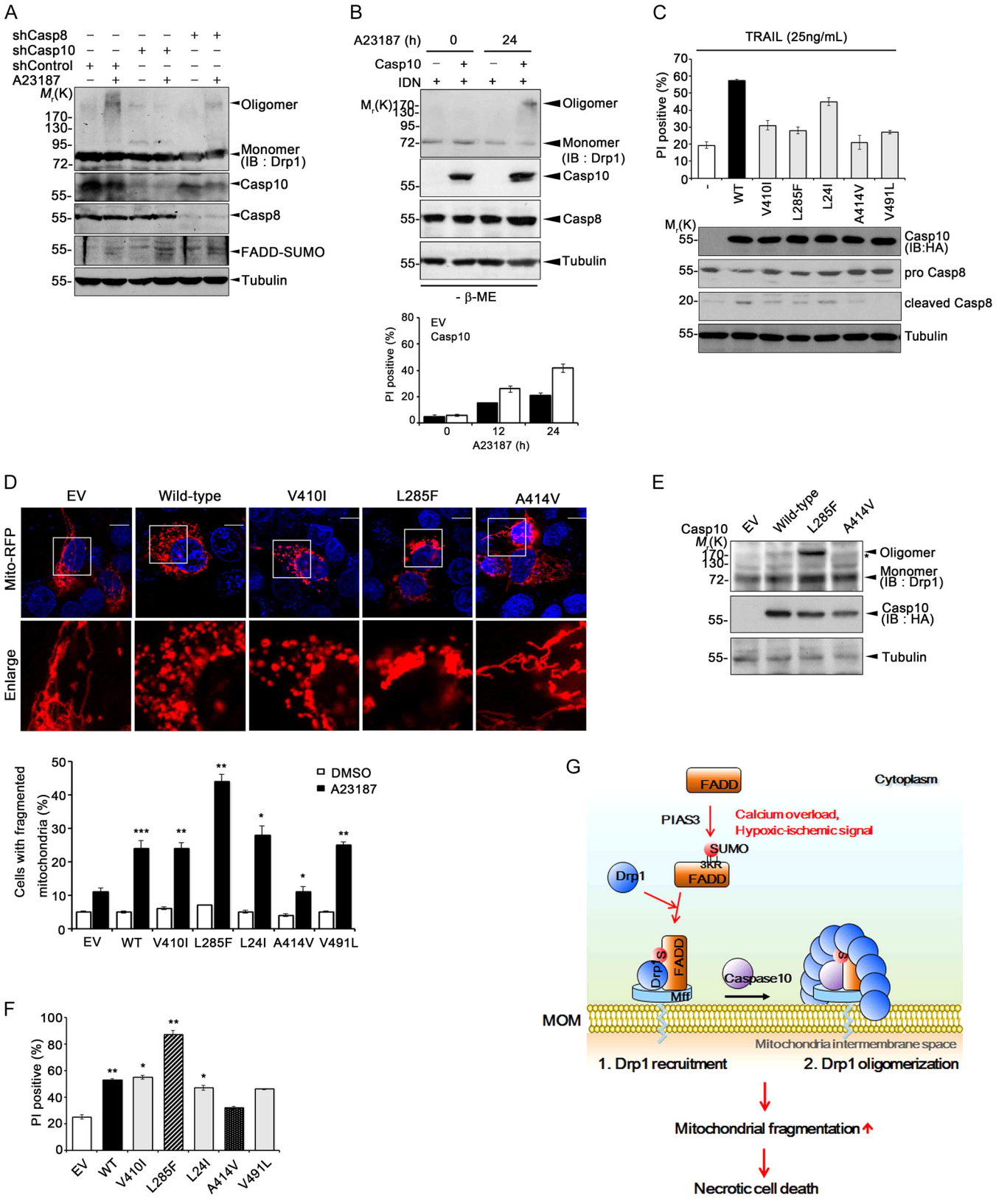

FIG 7 Caspase-10 L285F and A414V mutants detected in human diseases differentially regulate necrosis through affecting Drp1 oligomerization. (A) HeLa cells were transfected with caspase-10 shRNA or caspase-8 shRNA for 48 h. After treatment with 10 μM A23187 for 6 h, the mitochondrial fraction was subjected to immunoblotting under nonreducing conditions. (B) MCF-7 cells were transfected with pcDNA (−) or caspase-10 (+) for 24 h and treated with 20 μM A23187 for the indicated times. (Top) Cell extracts were subjected to immunoblotting under nonreducing conditions. (Bottom) Cell death rates were determined by staining with PI. (C) (Top) MCF-7 cells were transfected with GFP and pcDNA (−), caspase-10 WT, or one of the caspase-10 mutants (either V410I, L285F, L24I,

(Continued on next page)

requires Drp1. In general, Drp1-mediated mitochondrial fission is a widespread phenomenon observed in the processes of apoptosis and necrosis. During apoptosis, Drp1-induced fission is related to mitochondrial outer membrane permeabilization, cytochrome *c* release, and caspase activation. For necrosis, unbalanced mitochondrial fission leads to ATP depletion, mitochondrial clustering around nuclei, and cell rupture. Nevertheless, mitochondrial-fission-associated necrosis is poorly understood. Our results have uncovered a mechanism of regulated necrosis in which Drp1-dependent necrosis is under the control of FADD. This finding is highlighted by the fact that SUMOylated FADD physically interacts with Drp1. The resulting FADD/Drp1 complex translocates to the mitochondria for mitochondrial-fragmentation-mediated necrosis. While recent evidence has shown that Drp1 triggers necrosis through opening the MPTP either under ischemic/reperfusion conditions (45) or independently (46), we scarcely observed the opening of MPTPs during necrosis triggered by A23187 treatment.

During ischemic stroke, ischemic cores, where brain regions sustain severely impaired blood flow, undergo necrotic cell death; this is in contrast with the ischemic penumbra, which is prone to apoptosis (47). In the ischemic core, reduced ATP production increases intracellular calcium levels by opening two glutamate ionotropic receptors to trigger necrotic cell death in neurons. In an MCAO model, our observations that FADD was SUMOylated and interacted with Drp1 in the ischemic damage core provide a molecular mechanism underlying the necrotic damage that occurs within the ischemic core. In nonexcitable HeLa cells, hypoxia-induced calcium influx is unclear, but we found that hypoxia-induced cell death was suppressed by a calcium chelator. Future challenges involve investigating FADD SUMOylation in other types of necrotic cell death and in many pathophysiologic conditions, such as a transgenic mouse model of Huntington's disease, cerulein-induced pancreatitis, and myocardial infarction (48–50).

Surprisingly, caspase-10, but not caspase-8, is critical in SUMO-FADD/Drp1-mediated necrosis. Despite many studies, the functional differences between these two proximal caspases occurring in humans remain unclear. In general, caspase-8 mediates extrinsic apoptosis, so that caspase-8 deficiency is enough to block cell death. In our study, caspase-10 bound to only SUMOylated FADD/Drp1 to execute regulated necrosis, during which caspase-10 seemed to modulate Drp1 oligomerization. Recent studies demonstrated the role of Mff in the oligomerization of Drp1. Drp1 itself undergoes self-assembly via the middle and GED domains, and this assembly is stimulated by the presence of Mff at the membrane via the formation of extended filamentous structures (51, 52). Caspase-10 is also known to be activated by self-aggregation and to associate with signaling molecules through the death effector domain (DED) and the DD (53). Therefore, the oligomerization of Drp1 can be influenced by the properties of caspase-10 to form oligomers. Like Mff, the binding of caspase-10 to Drp1 might also trigger conformational changes of Drp1 to promote Drp1 oligomerization. Furthermore, the variable domain (VD) that resides between the middle domain and the GED domain of Drp1 has been shown to have a role in the regulation of Drp1 oligomerization. The VD contains multiple SUMOylation sites and two phosphorylation sites. Among them, phosphorylation of serine 616 inhibits Drp1 oligomerization (54). Thus, the interaction between caspase-10 and Drp1 may affect the oligomerization of Drp1 by disrupting such posttranslational modifications. Of course, there might be more factors that alter the assembly properties of Drp1 for mitochondrial fission.

FIG 7 Legend (Continued)
A414V, or V491L) for 24 h. The cells were then treated with 25 ng/ml TRAIL for 8 h, and cell death rates were determined by staining with PI. (Bottom) Cell extracts were examined by Western blotting. (D) MCF-7 cells were cotransfected with mito-RFP and pcDNA (EV), caspase-10 WT, or a caspase-10 mutant for 24 h. After treatment with 20 μM A23187 for 12 h, mitochondrial fragmentation was observed with a confocal microscope (top), and the percentages of T cells showing mitochondrial fragmentation in each group were determined (bottom). *, $P < 0.05$; **, $P < 0.01$, ***, $P < 0.001$. Scale bars, 10 μm. (E and F) MCF7 cells were transfected with pcDNA (EV), caspase-10 WT, or caspase-10 mutant for 24 h and treated with 20 μM A23187 for 12 h (E) or 24 h (F). Cell extracts were subjected to immunoblotting under nonreducing conditions (E), or cell death rates were determined by staining with PI (F). *, $P < 0.05$; **, $P < 0.01$. (G) FADD is SUMOylated on three lysines under calcium stress, and the resulting SUMOylated FADD binds to Drp1 to recruit it to the mitochondria. Caspase-10 forms a protein complex with SUMO-FADD/Drp1 and its activity-independent function stimulates Drp1 oligomerization for mitochondrial fragmentation during regulated necrosis. Shown are mean values and SD ($n \geq 3$).

In the mouse, there is only one proximal caspase that generally shares its apoptotic activity characteristics with human caspase-8. However, the presence of this signaling pathway employing SUMOylated FADD/Drp1/caspase in the mouse MCAO model and in MEFs implies that a murine proximal caspase might also have properties similar to human caspase-10, at least for this type of cell death (55–57). More interestingly, this function of caspase-10 was independent of its enzymatic activity and was differentially affected by the caspase-10 mutations identified in human diseases. Notably, the caspase-10 A414V and L285F mutations are exclusively found in non-Hodgkin lymphoma (30% of total cancers) and ALPS, respectively. Until now, the pathophysiological significance of these mutations has been interpreted only within the context of apoptosis. However, the notion that necrosis is highly implicated in inflammation in many disease models leads us to speculate that caspase-10 mutations, such as caspase-10 A414V and caspase-10 L285F, may contribute to pathogenesis through our working model of SUMO-FADD-mediated necrosis (Fig. 7G).

In summary, we have identified a novel pathway of regulated necrosis that utilizes SUMOylated FADD and caspase-10 and regulates Drp1-mediated mitochondrial fragmentation. In particular, FADD SUMOylation is crucial during necrosis under calcium overload and hypoxic/ischemic conditions. This promises to provide many insights into the development of new therapeutic modalities.

MATERIALS AND METHODS

The full experimental procedures are described in the supplemental material.

Cell culture and antibodies. Cells were cultured in Dulbecco's modified Eagle's medium (DMEM) (HyClone) supplemented with 10% fetal bovine serum (FBS) (HyClone). Drp1 knockout MEFs and FADD knockout MEFs were kind gifts from K. Mihara (Kyushu University, Japan) and J. Chang (Thomas Jefferson University), respectively. The antibodies used in this study are described in the supplemental material. Transfection was carried out with Lipofectamine (Invitrogen), Polyfect reagent (Qiagen), or PEI (Sigma), following the manufacturers' instructions.

Measurement of cell death. Cells were stained with PI (1 μg/ml), after which necrotic cell death was assessed by counting the PI-positive cells showing plasma membrane destruction and ruptured morphology (>300 cells) under a fluorescence microscope (Olympus).

Assays for SUMOylation. HA-FADD, Flag-Ubc9, and His-SUMOs were overexpressed in HEK293T cells together with one of the PIASs. Cell lysates in denaturing buffer (5% SDS) were incubated with Ni^{2+}-NTA-agarose (Qiagen), and the bound proteins were resolved by immunoblot analysis. For assaying SUMOylation of endogenous FADD, cell lysates were incubated with FADD antibody (G-4) overnight at 4°C and then with protein G-Sepharose (GE Healthcare). For *in vitro* SUMOylation assays, purified GB1-FADD (2 mg), SUMO2 (2 mg), SAE1/SAE2 (0.5 mg), and Ubc9 (1 mg) proteins were incubated in 50 mM Tris-HCl (pH 7.5) containing 5 mM $MgCl_2$ and 2 mM ATP. For *E. coli* SUMOylation, pET-FADD and pTE1E2S1 or pTE1E2S2 were transformed into strain BL21(DE3), and bacterial cultures were treated with 1 mM IPTG for 5 h at 25°C.

Isolation of mitochondrion-enriched fraction. Cells were subjected to sonication with an Ultrasonic Processor 130 W (Sonics and Materials) in buffer A (250 mM sucrose, 20 mM HEPES-NaOH [pH 7.5], 2 mM EGTA [pH 7.2], 10 mM KCl, 1.5 mM $MgCl_2$) at 4°C. After brief centrifugation at 1,000 $\times$ *g* for 10 min at 4°C, the mitochondrial pellet was obtained by further centrifugation at 10,000 $\times$ *g* for 15 min, washed with buffer B (1 mM EDTA, 10 mM Tris-HCl, pH 7.4), and spun at 10,000 $\times$ *g* again for 20 min at 4°C (mitochondrion-rich fraction).

Measurement of the ATP level. Cells were lysed with 1$\times$ lysis buffer (Promega). After cooling in ice for 10 min, the cell lysates were centrifuged (12,000 rpm at 4°C for 10 min), and the supernatant (50 μl) was mixed with rL/L ATP substrate (50 μl) (Promega). The ATP bioluminescence of the reaction mixture was measured immediately using a luminometer.

Model of MCAO. C57BL/6 mice (12-week-old males; 20 to 25 g) were anesthetized with a PBS-zoletil-rompun mixture (60%:35%:5%) during surgical preparation by intraperitoneal injection. The right common carotid artery was isolated, and a size 6-0 microfilament with a silicon rubber-coated tip (diameter, 0.21 mm; Doccol Corporation) was inserted into the right MCA. After 30 min, the mice were sacrificed or followed by reperfusion for 2 h by withdrawing the suture. Sham-operation mice underwent the same procedure except for MCA blocking.

Statistical analyses. All statistical analyses were performed using a two-tailed Student *t* test or one-way analysis of variance (ANOVA), following densitometric analysis with SigmaStat software.

SUPPLEMENTAL MATERIAL

Supplemental material for this article may be found at https://doi.org/10.1128/MCB.00254-16.

TEXT S1, PDF file, 4.7 MB.

ACKNOWLEDGMENTS

We thank K. Mihara (Kyushu University, Japan) for Drp1 wild-type and knockout MEFs, J. Chang (Thomas Jefferson University) for FADD wild-type and knockout MEFs, and M. T. Ryan (LaTrobe University, Australia) for Fis1, Mff, MiD49, and MiD51.

This work was supported by the Global Research Laboratory (NRF-2010-00341) and a CRI grant (NRF-2016R1A2A1A05005304) funded by the Ministry of Education, Science, and Technology.

Seon-Guk Choi, Hyunjoo Kim, and Ho-June Lee performed mutagenesis, immunoprecipitation assays, and cell line characterization. Seon-Guk Choi and Eun Il Jeong performed myocardial artery occlusion. Seon-Guk Choi and Sungwoo Park performed subcellular fractionation and mitochondrial fragmentation assays. Seon-Guk Choi, Hyunjoo Kim, Song-Yi Lee, and Hyeon-Jeong Lee examined modification of FADD under necrotic stimuli. Seon-Guk Choi, Ho-June Lee, and Seong Won Lee performed *in vitro* and *in vivo* SUMOylation assays. Yong-Keun Jung and Chin Ha Chung guided the project and data interpretation. Seon-Guk Choi and Yong-Keun Jung wrote the manuscript.

REFERENCES

1. Kim H, Lee HJ, Oh Y, Choi SG, Hong SH, Kim HJ, Lee SY, Choi JW, Su Hwang D, Kim KS, Kim HJ, Zhang J, Youn HJ, Noh DY, Jung YK. 2014. The DUSP26 phosphatase activator adenylate kinase 2 regulates FADD phosphorylation and cell growth. Nat Commun 5:3351. https://doi.org/10.1038/ncomms4351.
2. Lee EW, Kim JH, Ahn YH, Seo J, Ko A, Jeong M, Kim SJ, Ro JY, Park KM, Lee HW, Park EJ, Chun KH, Song J. 2012. Ubiquitination and degradation of the FADD adaptor protein regulate death receptor-mediated apoptosis and necroptosis. Nat Commun 3:978. https://doi.org/10.1038/ncomms1981.
3. Kawahara A, Ohsawa Y, Matsumura H, Uchiyama Y, Nagata S. 1998. Caspase-independent cell killing by Fas-associated protein with death domain. J Cell Biol 143:1353–1360. https://doi.org/10.1083/jcb.143.5.1353.
4. Matsumura H, Shimizu Y, Ohsawa Y, Kawahara A, Uchiyama Y, Nagata S. 2000. Necrotic death pathway in Fas receptor signaling. J Cell Biol 151:1247–1256. https://doi.org/10.1083/jcb.151.6.1247.
5. Juo P, Kuo CJ, Yuan J, Blenis J. 1998. Essential requirement for caspase-8/FLICE in the initiation of the Fas-induced apoptotic cascade. Curr Biol 8:1001–1008. https://doi.org/10.1016/S0960-9822(07)00420-4.
6. Teitz T, Wei T, Valentine MB, Vanin EF, Grenet J, Valentine VA, Behm FG, Look AT, Lahti JM, Kidd VJ. 2000. Caspase 8 is deleted or silenced preferentially in childhood neuroblastomas with amplification of MYCN. Nat Med 6:529–535. https://doi.org/10.1038/75007.
7. Lee HJ, Pyo JO, Oh Y, Kim HJ, Hong SH, Jeon YJ, Kim H, Cho DH, Woo HN, Song S, Nam JH, Kim HJ, Kim KS, Jung YK. 2007. AK2 activates a novel apoptotic pathway through formation of a complex with FADD and caspase-10. Nat Cell Biol 9:1303–1310. https://doi.org/10.1038/ncb1650.
8. Lamy L, Ngo VN, Emre NC, Shaffer AL III, Yang Y, Tian E, Nair V, Kruhlak MJ, Zingone A, Landgren O, Staudt LM. 2013. Control of autophagic cell death by caspase-10 in multiple myeloma. Cancer Cell 23:435–449. https://doi.org/10.1016/j.ccr.2013.02.017.
9. Chaudhary PM, Eby MT, Jasmin A, Kumar A, Liu L, Hood L. 2000. Activation of the NF-kappaB pathway by caspase 8 and its homologs. Oncogene 19:4451–4460. https://doi.org/10.1038/sj.onc.1203812.
10. Harada K, Toyooka S, Shivapurkar N, Maitra A, Reddy JL, Matta H, Miyajima K, Timmons CF, Tomlinson GE, Mastrangelo D, Hay RJ, Chaudhary PM, Gazdar AF. 2002. Deregulation of caspase 8 and 10 expression in pediatric tumors and cell lines. Cancer Res 62:5897–5901.
11. Park WS, Lee JH, Shin MS, Park JY, Kim HS, Lee JH, Kim YS, Lee SN, Xiao W, Park CH, Lee SH, Yoo NJ, Lee JY. 2002. Inactivating mutations of the caspase-10 gene in gastric cancer. Oncogene 21:2919–2925. https://doi.org/10.1038/sj.onc.1205394.
12. Shin MS, Kim HS, Kang CS, Park WS, Kim SY, Lee SN, Lee JH, Park JY, Jang JJ, Kim CW, Kim SH, Lee JY, Yoo NJ, Lee SH. 2002. Inactivating mutations of CASP10 gene in non-Hodgkin lymphomas. Blood 99:4094–4099. https://doi.org/10.1182/blood.V99.11.4094.
13. Wang J, Zheng L, Lobito A, Chan FK, Dale J, Sneller M, Yao X, Puck JM, Straus SE, Lenardo MJ. 1999. Inherited human Caspase 10 mutations underlie defective lymphocyte and dendritic cell apoptosis in autoimmune lymphoproliferative syndrome type II. Cell 98:47–58. https://doi.org/10.1016/S0092-8674(00)80605-4.
14. Vaseva AV, Marchenko ND, Ji K, Tsirka SE, Holzmann S, Moll UM. 2012. p53 opens the mitochondrial permeability transition pore to trigger necrosis. Cell 149:1536–1548. https://doi.org/10.1016/j.cell.2012.05.014.
15. Wang Z, Jiang H, Chen S, Du F, Wang X. 2012. The mitochondrial phosphatase PGAM5 functions at the convergence point of multiple necrotic death pathways. Cell 148:228–243. https://doi.org/10.1016/j.cell.2011.11.030.
16. Gustafsson AB, Gottlieb RA. 2008. Heart mitochondria: gates of life and death. Cardiovasc Res 77:334–343.
17. Shirendeb U, Reddy AP, Manczak M, Calkins MJ, Mao P, Tagle DA, Reddy PH. 2011. Abnormal mitochondrial dynamics, mitochondrial loss and mutant Huntingtin oligomers in Huntington's disease: implications for selective neuronal damage. Hum Mol Genet 20:1438–1455. https://doi.org/10.1093/hmg/ddr024.
18. Mears JA, Lackner LL, Fang S, Ingerman E, Nunnari J, Hinshaw JE. 2011. Conformational changes in Dnm1 support a contractile mechanism for mitochondrial fission. Nat Struct Mol Biol 18:20–26. https://doi.org/10.1038/nsmb.1949.
19. Otera H, Ishihara N, Mihara K. 2013. New insights into the function and regulation of mitochondrial fission. Biochim Biophys Acta 1833:1256–1268. https://doi.org/10.1016/j.bbamcr.2013.02.002.
20. Liu T, Roh SE, Woo JA, Ryu H, Kang DE. 2013. Cooperative role of RanBP9 and P73 in mitochondria-mediated apoptosis. Cell Death Dis 4:e476. https://doi.org/10.1038/cddis.2012.203.
21. Iglewski M, Hill JA, Lavandero S, Rothermel BA. 2010. Mitochondrial fission and autophagy in the normal and diseased heart. Curr Hypertens Rep 12:418–425. https://doi.org/10.1007/s11906-010-0147-x.
22. Whelan RS, Konstantinidis K, Wei AC, Chen Y, Reyna DE, Jha S, Yang Y, Calvert JW, Lindsten T, Thompson CB, Crow MT, Gavathiotis E, Dorn GW II, O'Rourke B, Kitsis RN. 2012. Bax regulates primary necrosis through mitochondrial dynamics. Proc Natl Acad Sci U S A 109:6566–6571. https://doi.org/10.1073/pnas.1201608109.
23. Johnson ES. 2004. Protein modification by SUMO. Annu Rev Biochem 73:355–382. https://doi.org/10.1146/annurev.biochem.73.011303.074118.
24. Bischof O, Schwamborn K, Martin N, Werner A, Sustmann C, Grosschedl R, Dejean A. 2006. The E3 SUMO ligase PIASy is a regulator of cellular senescence and apoptosis. Mol Cell 22:783–794. https://doi.org/10.1016/j.molcel.2006.05.016.
25. Huang TT, Wuerzberger-Davis SM, Wu ZH, Miyamoto S. 2003. Sequential modification of NEMO/IKKgamma by SUMO-1 and ubiquitin mediates NF-kappaB activation by genotoxic stress. Cell 115:565–576. https://doi.org/10.1016/S0092-8674(03)00895-X.
26. Besnault-Mascard L, Leprince C, Auffredou MT, Meunier B, Bourgeade MF, Camonis J, Lorenzo HK, Vazquez A. 2005. Caspase-8 sumoylation is associated with nuclear localization. Oncogene 24:3268–3273. https://doi.org/10.1038/sj.onc.1208448.

27. Ren J, Gao X, Jin C, Zhu M, Wang X, Shaw A, Wen L, Yao X, Xue Y. 2009. Systematic study of protein sumoylation: development of a site-specific predictor of SUMOsp 2.0. Proteomics 9:3409–3412. https://doi.org/10.1002/pmic.200800646.
28. Uchimura Y, Nakao M, Saitoh H. 2004. Generation of SUMO-1 modified proteins in E. coli: towards understanding the biochemistry/structural biology of the SUMO-1 pathway. FEBS Lett 564:85–90. https://doi.org/10.1016/S0014-5793(04)00321-7.
29. Elmore S. 2007. Apoptosis: a review of programmed cell death. Toxicol Pathol 35:495–516. https://doi.org/10.1080/01926230701320337.
30. Endo H, Kamada H, Nito C, Nishi T, Chan PH. 2006. Mitochondrial translocation of p53 mediates release of cytochrome *c* and hippocampal CA1 neuronal death after transient global cerebral ischemia in rats. J Neurosci 26:7974–7983. https://doi.org/10.1523/JNEUROSCI.0897-06.2006.
31. Cereghetti GM, Stangherlin A, Martins de Brito O, Chang CR, Blackstone C, Bernardi P, Scorrano L. 2008. Dephosphorylation by calcineurin regulates translocation of Drp1 to mitochondria. Proc Natl Acad Sci U S A 105:15803–15808. https://doi.org/10.1073/pnas.0808249105.
32. Choi WS, Lee EH, Chung CW, Jung YK, Jin BK, Kim SU, Oh TH, Saido TC, Oh YJ. 2001. Cleavage of Bax is mediated by caspase-dependent or -independent calpain activation in dopaminergic neuronal cells: protective role of Bcl-2. J Neurochem 77:1531–1541. https://doi.org/10.1046/j.1471-4159.2001.00368.x.
33. Smirnova E, Griparic L, Shurland DL, van der Bliek AM. 2001. Dynamin-related protein Drp1 is required for mitochondrial division in mammalian cells. Mol Biol Cell 12:2245–2256. https://doi.org/10.1091/mbc.12.8.2245.
34. Breckenridge DG, Stojanovic M, Marcellus RC, Shore GC. 2003. Caspase cleavage product of BAP31 induces mitochondrial fission through endoplasmic reticulum calcium signals, enhancing cytochrome *c* release to the cytosol. J Cell Biol 160:1115–1127. https://doi.org/10.1083/jcb.200212059.
35. Choi DW. 1995. Calcium: still center-stage in hypoxic-ischemic neuronal death. Trends Neurosci 18:58–60. https://doi.org/10.1016/0166-2236(95)80018-W.
36. Bonfoco E, Krainc D, Ankarcrona M, Nicotera P, Lipton SA. 1995. Apoptosis and necrosis: two distinct events induced, respectively, by mild and intense insults with N-methyl-D-aspartate or nitric oxide/superoxide in cortical cell cultures. Proc Natl Acad Sci U S A 92:7162–7166. https://doi.org/10.1073/pnas.92.16.7162.
37. Kristian T, Siesjo BK. 1998. Calcium in ischemic cell death. Stroke 29:705–718. https://doi.org/10.1161/01.STR.29.3.705.
38. Shin HW, Takatsu H, Mukai H, Munekata E, Murakami K, Nakayama K. 1999. Intermolecular and interdomain interactions of a dynamin-related GTP-binding protein, Dnm1p/Vps1p-like protein. J Biol Chem 274:2780–2785. https://doi.org/10.1074/jbc.274.5.2780.
39. Sampson DA, Wang M, Matunis MJ. 2001. The small ubiquitin-like modifier-1 (SUMO-1) consensus sequence mediates Ubc9 binding and is essential for SUMO-1 modification. J Biol Chem 276:21664–21669. https://doi.org/10.1074/jbc.M100006200.
40. Gareau JR, Lima CD. 2010. The SUMO pathway: emerging mechanisms that shape specificity, conjugation and recognition. Nat Rev Mol Cell Biol 11:861–871. https://doi.org/10.1038/nrm3011.
41. Buschmann T, Fuchs SY, Lee CG, Pan ZQ, Ronai Z. 2000. SUMO-1 modification of Mdm2 prevents its self-ubiquitination and increases Mdm2 ability to ubiquitinate p53. Cell 101:753–762. https://doi.org/10.1016/S0092-8674(00)80887-9.
42. Meinecke I, Cinski A, Baier A, Peters MA, Dankbar B, Wille A, Drynda A, Mendoza H, Gay RE, Hay RT, Ink B, Gay S, Pap T. 2007. Modification of nuclear PML protein by SUMO-1 regulates Fas-induced apoptosis in rheumatoid arthritis synovial fibroblasts. Proc Natl Acad Sci U S A 104:5073–5078. https://doi.org/10.1073/pnas.0608773104.
43. Babic I, Cherry E, Fujita DJ. 2006. SUMO modification of Sam68 enhances its ability to repress cyclin D1 expression and inhibits its ability to induce apoptosis. Oncogene 25:4955–4964. https://doi.org/10.1038/sj.onc.1209504.
44. Carneiro LA, Travassos LH, Soares F, Tattoli I, Magalhaes JG, Bozza MT, Plotkowski MC, Sansonetti PJ, Molkentin JD, Philpott DJ, Girardin SE. 2009. Shigella induces mitochondrial dysfunction and cell death in nonmyeloid cells. Cell Host Microbe 5:123–136. https://doi.org/10.1016/j.chom.2008.12.011.
45. Guo X, Sesaki H, Qi X. 2014. Drp1 stabilizes p53 on the mitochondria to trigger necrosis under oxidative stress conditions in vitro and in vivo. Biochem J 461:137–146. https://doi.org/10.1042/BJ20131438.
46. Hamahata K, Adachi S, Matsubara H, Okada M, Imai T, Watanabe K, Toyokuni SY, Ueno M, Wakabayashi S, Katanosaka Y, Akiba S, Kubota M, Nakahata T. 2005. Mitochondrial dysfunction is related to necrosis-like programmed cell death induced by A23187 in CEM cells. Eur J Pharmacol 516:187–196. https://doi.org/10.1016/j.ejphar.2005.04.018.
47. Markus R, Reutens DC, Kazui S, Read S, Wright P, Pearce DC, Tochon-Danguy HJ, Sachinidis JI, Donnan GA. 2004. Hypoxic tissue in ischaemic stroke: persistence and clinical consequences of spontaneous survival. Brain 127:1427–1436. https://doi.org/10.1093/brain/awh162.
48. Chen X, Wu J, Lvovskaya S, Herndon E, Supnet C, Bezprozvanny I. 2011. Dantrolene is neuroprotective in Huntington's disease transgenic mouse model. Mol Neurodegener 6:81. https://doi.org/10.1186/1750-1326-6-81.
49. Orabi AI, Shah AU, Ahmad MU, Choo-Wing R, Parness J, Jain D, Bhandari V, Husain SZ. 2010. Dantrolene mitigates caerulein-induced pancreatitis in vivo in mice. Am J Physiol Gastrointest Liver Physiol 299:G196–G204. https://doi.org/10.1152/ajpgi.00498.2009.
50. Yu G, Zucchi R, Ronca-Testoni S, Ronca G. 2000. Protection of ischemic rat heart by dantrolene, an antagonist of the sarcoplasmic reticulum calcium release channel. Basic Res Cardiol 95:137–143. https://doi.org/10.1007/s003950050175.
51. Clinton RW, Francy CA, Ramachandran R, Qi X, Mears JA. 2016. Dynamin-related protein 1 oligomerization in solution impairs functional interactions with membrane-anchored mitochondrial fission factor. J Biol Chem 291:478–492. https://doi.org/10.1074/jbc.M115.680025.
52. Strack S, Cribbs JT. 2012. Allosteric modulation of Drp1 mechanoenzyme assembly and mitochondrial fission by the variable domain. J Biol Chem 287:10990–11001. https://doi.org/10.1074/jbc.M112.342105.
53. Wang J, Chun HJ, Wong W, Spencer DM, Lenardo MJ. 2001. Caspase-10 is an initiator caspase in death receptor signaling. Proc Natl Acad Sci U S A 98:13884–13888. https://doi.org/10.1073/pnas.241358198.
54. Cho B, Cho HM, Kim HJ, Jeong J, Park SK, Hwang EM, Park JY, Kim WR, Kim H, Sun W. 2014. CDK5-dependent inhibitory phosphorylation of Drp1 during neuronal maturation. Exp Mol Med 46:e105. https://doi.org/10.1038/emm.2014.36.
55. Stupack DG, Teitz T, Potter MD, Mikolon D, Houghton PJ, Kidd VJ, Lahti JM, Cheresh DA. 2006. Potentiation of neuroblastoma metastasis by loss of caspase-8. Nature 439:95–99. https://doi.org/10.1038/nature04323.
56. Giampietri C, Petrungaro S, Coluccia P, D'Alessio A, Starace D, Riccioli A, Padula F, Srinivasula SM, Alnemri E, Palombi F, Filippini A, Ziparo E, De Cesaris P. 2003. FLIP is expressed in mouse testis and protects germ cells from apoptosis. Cell Death Differ 10:175–184. https://doi.org/10.1038/sj.cdd.4401137.
57. Garcia-Calvo M, Peterson EP, Leiting B, Ruel R, Nicholson DW, Thornberry NA. 1998. Inhibition of human caspases by peptide-based and macromolecular inhibitors. J Biol Chem 273:32608–32613. https://doi.org/10.1074/jbc.273.49.32608.